BRIEF COMMUNICATION www.jasn.org

Fibroblasts in Kidney Fibrosis Emerge *via* Endothelial-to-Mesenchymal Transition

Elisabeth M. Zeisberg,* Scott E. Potenta,* Hikaru Sugimoto,* Michael Zeisberg,* and Raghu Kalluri*†‡

*Division of Matrix Biology, Department of Medicine, Beth Israel Deaconess Medical Center and Harvard Medical School, †Department of Biological Chemistry and Molecular Pharmacology, and ‡Harvard-MIT Division of Health Sciences and Technology, Boston, Massachusetts

ABSTRACT

Fibroblasts are key mediators of fibrosis in the kidney and other organs, but their origin during fibrosis is still not completely clear. Activated fibroblasts likely arise from resident quiescent fibroblasts *via* epithelial-to-mesenchymal transition and from the bone marrow. Here, we demonstrate that endothelial cells also contribute to the emergence of fibroblasts during kidney fibrosis *via* the process of endothelial-to-mesenchymal transition (EndMT). We examined the contribution of EndMT to renal fibrosis in three mouse models of chronic kidney disease: (*1*) Unilateral ureteral obstructive nephropathy, (*2*) streptozotocin-induced diabetic nephropathy, and (*3*) a model of Alport renal disease. Approximately 30 to 50% of fibroblasts coexpressed the endothelial marker CD31 and markers of fibroblasts and myofibroblasts such as fibroblast specific protein-1 and α-smooth muscle actin. Endothelial lineage tracing using *Tie2-Cre;R26R-stop-EYFP* transgenic mice further confirmed the presence of EndMT-derived fibroblasts. Collectively, our results demonstrate that EndMT contributes to the accumulation of activated fibroblasts and myofibroblasts in kidney fibrosis and suggest that targeting EndMT might have therapeutic potential.

J Am Soc Nephrol 19: 2282–2287, 2008. doi: 10.1681/ASN.2008050513

Chronic kidney disease (CKD) leading to end-stage kidney failure is associated with interstitial kidney fibrosis regardless of the underlying cause.[1] As of now, there are no specific treatments to target fibrosis in the clinic.[1,2] Interstitial renal fibrosis is characterized by tubular atrophy/dilation, interstitial leukocyte infiltration, accumulation of fibroblasts, and increased interstitial matrix deposition.[3] Although many different cell types are involved, fibroblasts are considered to be the key mediators of fibrosis in the kidney and in other organs.[4,5]

Kidney fibrosis is a good model system for studying the source of activated fibroblasts. Although for many years a common notion was that activated fibroblasts arise primarily from resident fibroblasts, recent evidence has demonstrated that during fibrosis, activated fibroblasts can also arise from epithelial cells *via* epithelial-to-mesenchymal transition (EMT) and can be recruited from the bone marrow.[6] In addition to these mechanisms of recruiting activated fibroblasts, we recently demonstrated that endothelial-to-mesenchymal transition (EndMT) plays a significant role in cardiac fibrosis and also in the recruitment of carcinoma-associated fibroblasts.[7,8] EndMT was first described during embryonic heart development, where mesenchymal cells of the endocardial cushion (a tissue that later gives rise to the cardiac septa and valves) arise from endothelial cells of the endocardium.[9] Here we addressed the question of whether EndMT contributes to fibroblast accumulation in kidney fibrosis.

In this study, we explored the contribution of EndMT to renal fibrosis in three independent mouse models of CKD: (*1*) A mouse model of unilateral ureteral obstruction (UUO; a model of obstructive nephropathy), (*2*) a model of streptozotocin-induced diabetic nephropathy, and (*3*) mice that systemically lack the collagen IV α3 chain (COL4A3 KO; a mouse model for Alport disease). Here we report that in all three mouse models, a considerable portion of activated fibroblasts coexpress the endothelial marker CD31, indicating that these fibroblasts likely carry an endothelial imprint. In the UUO model, endothelial lineage tracing using *Tie2-Cre; R26R-stop-EYFP* transgenic mice revealed yellow fluorescence protein (YFP) expression in a substantial portion of activated fibroblasts, thereby confirming the endothelial origin of these fibroblasts. To our

Received May 19, 2008. Accepted August 18, 2008.

Published online ahead of print. Publication date available at www.jasn.org.

E.M.Z. and S.E.P. contributed equally to this work and should be considered co-first authors.

Correspondence: Dr. Raghu Kalluri, Department of Medicine, Harvard Medical School, Division of Matrix Biology, Department of Medicine, CLS 11086, Beth Israel Deaconess Medical Center, 330 Brookline Avenue, 3 Blackfan Circle, Boston, MA 02215. Phone: 617-735-4601; Fax: 617-735-4602; E-mail: rkalluri@bidmc.harvard.edu

knowledge, this is the first report demonstrating that EndMT is a possible contributor to the accumulation of activated fibroblasts in kidney fibrosis. These findings have far-reaching implications, raising the possibility that inhibiting EndMT may be an effective therapy for delaying the progression of fibrosis associated with CKD.

Using genetic lineage tracing of endothelial cells and double labeling of tissue for endothelial and fibroblast markers, we previously demonstrated that co-labeling of tissue with the endothelial marker CD31 and the fibroblast markers α-smooth muscle actin (α-SMA) and fibroblast-specific protein 1 (FSP1) reliably identifies fibroblasts derived *via* EndMT.[7] Furthermore, FSP1 and α-SMA identify distinct fibroblast populations with only few fibroblasts carrying both markers at the same time.[7,8] Here we performed endothelial lineage tracing and FSP1/CD31 and α-SMA/CD31 double-labeling experiments to gain insights into possible EndMT in renal fibrogenesis. We first analyzed EndMT in the setting of UUO, a model of obstructive nephropathy.[10] This model is well studied with regard to the origin of fibroblasts during fibrosis.[6] Furthermore, TGF-β has been implicated in the development of renal fibrosis induced by UUO and is a known inducer of EndMT in cardiac endothelial cells.[11] Smad3 deficiency has been shown to attenuate renal fibrosis after UUO, and in this regard Smad3 deficiency has also been shown to attenuate EndMT in the context of cardiac fibrosis.[11] In addition to the proliferation of fibroblasts, injury to the peritubular capillary network of the kidney is considered to be a key factor in the resulting pathology after UUO.[12] On the basis of these studies, we sought to test our hypothesis that the UUO model of kidney fibrosis is associated with EndMT.

We performed UUO in CD1 mice and confirmed mild interstitial fibrosis by Masson Trichrome staining (MTS) 1 wk after disease induction (Figure 1A). Both the FSP1-positive and α-SMA–positive fibroblast populations were substantially increased in kidneys with UUO as compared with sham-operated controls (Figure 1, B and C). To identify fibroblasts of endothelial origin, we performed double stainings for FSP1 and the endothelial marker CD31 and also for α-SMA and CD31. Although there was variability in the number of double-positive cells among different UUO mice, an average of 36% of all FSP1-positive fibroblasts and 25% of all α-SMA–positive fibroblasts coexpressed CD31. (Figure 1, B and C). To confirm the endothelial origin of these fibroblasts, we further performed UUO in *Tie2-Cre;R26R-stop-EYFP* mice. In these mice, cells of endothelial origin are irreversibly labeled with YFP, regardless of any subsequent phenotypic changes these cells may undergo. Staining with FSP1 and α-SMA revealed coexpression of YFP in a substantial portion of FSP1-positive fibroblasts and, albeit to a lesser extent, in α-SMA–positive fibroblasts (Figure 1D). These findings suggest that EndMT may account for a considerable portion of the fibroblasts in the mouse model of obstructive nephropathy.

Diabetic nephropathy is currently the most common cause of ESRD in the world.[13] Aside from glomerular hypertrophy, diffuse glomerulosclerosis, and tubular atrophy, interstitial fibrosis is one of the most prominent histopathologic lesions seen in patients with diabetic nephropathy. Recently, we described a new mouse model that mimics human diabetic nephropathy in many respects.[14] CD1 mice develop ESRD associated with prominent tubulointerstitial nephritis and fibrosis within 3 mo and subsequently die as a result of diabetic complications by 6 to 7 mo after a single injection of streptozotocin (STZ).[14] We analyzed kidneys 6 mo after injection of STZ and confirmed tubulointerstitial fibrosis by MTS (Figure 2A). We next evaluated FSP1-positive and α-SMA–positive fibroblasts and found a substantial increase of both FSP1-positive fibroblasts and of α-SMA–positive fibroblasts in STZ-treated kidneys compared with untreated controls (Figure 2, B and C). Double staining of these fibroblasts with CD31 further revealed that approximately 40% of all FSP1-positive cells and 50% of the α-SMA–positive cells in STZ kidneys were also CD31 positive, suggesting that these fibroblasts are likely of endothelial origin (Figure 2, B and C).

Next, we analyzed a third model of renal fibrosis to test our hypothesis that EndMT can occur in kidney fibrosis regardless of the underlying insult. *COL4A3 KO* mice develop proteinuria, glomerulonephritis, and subsequent tubulointerstitial fibrosis starting at 8 wk of age and eventually die from renal failure at approximately 20 to 23 wk of age.[15] We evaluated kidneys of 22-wk-old *COL4A3 KO* mice in this study. MTS revealed robust collagen deposition in the kidneys and a disrupted renal architecture (Figure 3A). The numbers of α-SMA–positive and FSP1-positive fibroblasts were considerably higher compared with wild-type mice, corresponding to the robust fibrosis (Figure 3, B and C). Coexpression of CD31 could be observed in 45% of all α-SMA–positive fibroblasts and 60% of all FSP1-positive fibroblasts, suggesting that EndMT may substantially contribute to the accumulation of fibroblasts in kidney fibrosis associated with *COL4A3 KO* mice (Figure 3, B and C).

To our knowledge, these results present the first evidence of possible EndMT in kidney fibrosis. Studies by Iwano *et al.*[16] in the UUO model of kidney fibrosis demonstrated that the sources of fibroblasts are likely manifold. While looking exclusively at the FSP1-positive fibroblast population, they demonstrated that 36% of all FSP1-positive cells derived from the epithelium *via* EMT and approximately 15% derived from the bone marrow. The remaining percentage, comprising approximately half of all FSP1-positive fibroblasts, was not accounted for in their study and was speculated to arise from proliferating resident fibroblasts. Our study complements the findings of Iwano *et al.*, because we report that 30 to 50% of all FSP1-positive fibroblasts arise from endothelial cells *via* EndMT; however, double labeling for mesenchymal and endothelial markers cannot detect EndMT-derived fibroblasts that have already lost endothelial markers. Therefore, the true percentage of EndMT-derived fibroblasts may be even higher. Interestingly, we detected a high percentage of EndMT-derived fibroblasts in the STZ model of diabetic nephropathy despite that the fibrosis was mild compared with the Alport mice (Figures 2A and 3A, right). The UUO model showed a similar amount of fibrosis when compared with the STZ model (Figures 1A and 2A, right), but the percentage of EndMT-derived fibroblasts

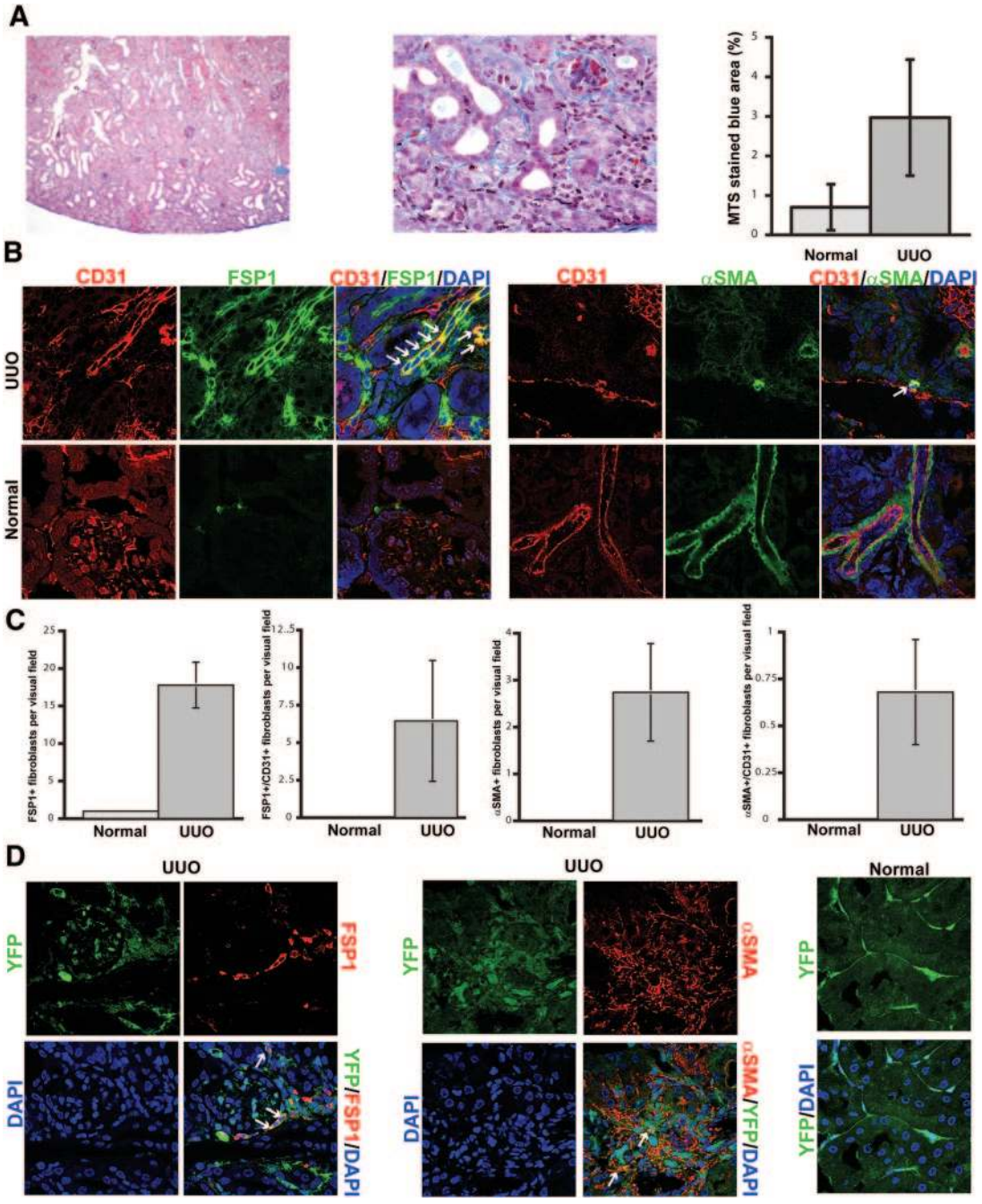

Figure 1. EndMT in the mouse model of UUO. (A) Kidneys were analyzed after 1 wk of ureter ligation. The pictures display representative photomicrographs of MTS-stained kidney section at an original magnification of ×10 (left) and ×60 (middle). Fibrosis was digitally quantified and is shown as the percentage of MTS-stained blue area in both normal and UUO kidneys (right). (B, left) FSP1 and CD31 double labeling. Frozen kidney sections were double stained with antibodies to FSP1 (green) and CD31 (red). DAPI was used as a nuclear stain (blue). The panels display representative images that were obtained from UUO kidneys (top) and normal kidneys (bottom) using a confocal microscope. The arrows in the merged panel point to $CD31^+FSP1^+$ cells. (B, right) α-SMA and CD31 double labeling. The pictures display representative pictures of kidneys that were labeled with antibodies to α-SMA (green) and CD31 (red). DAPI was used for labeling of nuclei (blue). Yellow color in the merged panel indicates coexpression of α-SMA and CD31. The photomicrographs were obtained by confocal microscopy. (C) Quantification of fibroblasts. The bar graphs summarize average numbers of $FSP1^+$ fibroblasts, $CD31^+FSP1^+$ cells, α-SMA^+ fibroblasts, and $CD31^+\alpha$-SMA^+ cells per visual field in both normal and obstructed kidneys at a magnification of ×63 ($n = 3$ mice per group, 10 high-power fields [hpf] per mouse, 30 hpf total). (D) Lineage tracing of endothelial cells. UUO was performed in *Tie2-Cre;R26R-stop-EYFP* double-transgenic mice. In this reporter strain, all cells of endothelial origin are tagged by YFP (shown in green). After UUO, immunostaining was performed for FSP1 (left, red) or α-SMA (middle, red). White arrows indicate fibroblasts of endothelial origin (yellow). For comparison, a representative YFP image from a normal *Tie2-Cre;R26R-stop-EYFP* kidney is also included (right). Magnification, ×63 in B and D.

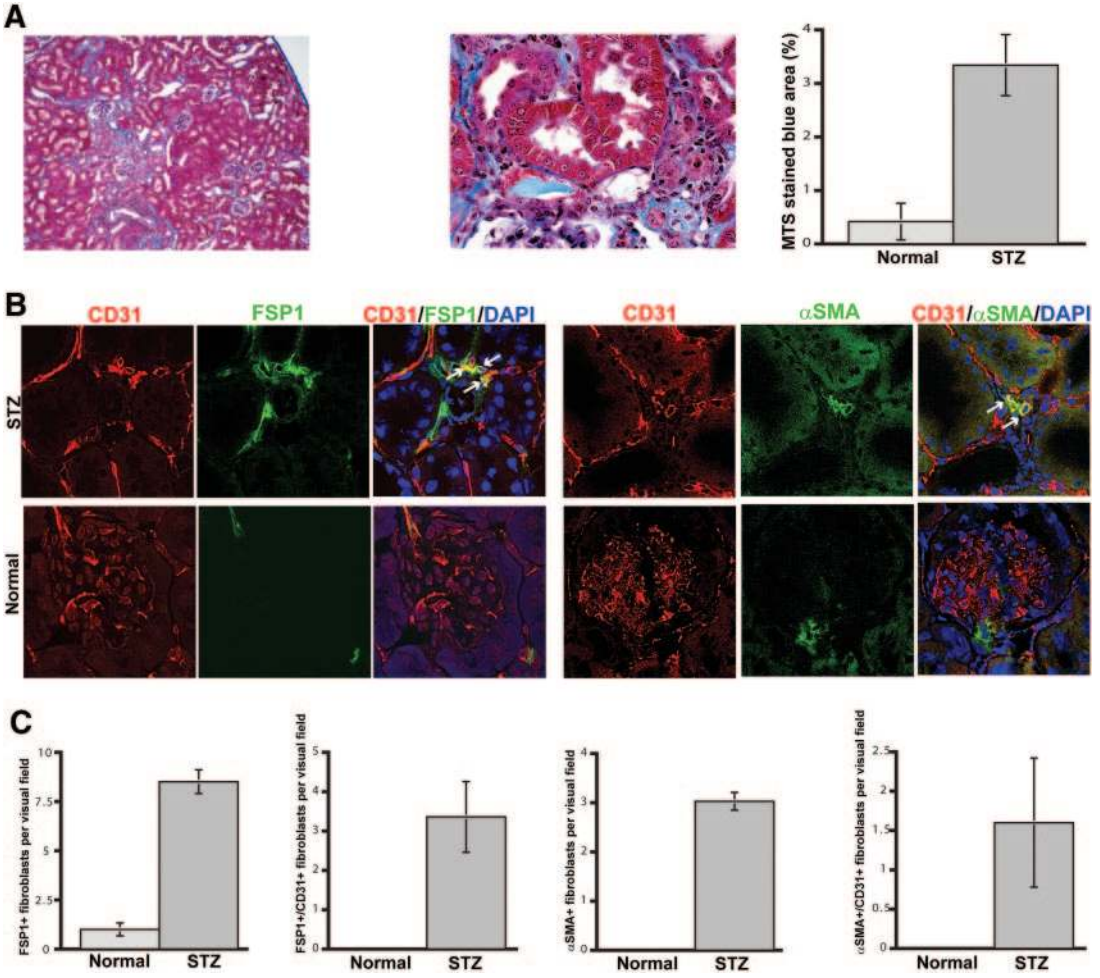

Figure 2. EndMT in the mouse model of STZ-induced diabetic nephropathy. (A) CD1 mice were made diabetic by a single injection of STZ. Kidneys were analyzed after 6 mo. The pictures display representative photomicrographs of MTS-stained kidney sections at an original magnification of ×10 (left) and ×60 (middle). Fibrosis was digitally quantified and is shown as the percentage of MTS-stained blue area in both normal and STZ kidneys (right). (B, left) FSP1 and CD31 double labeling. Frozen kidney sections were double stained with antibodies to FSP1 (green) and CD31 (red). DAPI was used to label the nuclei (blue). The panels display representative images that were obtained from STZ kidneys (top) and normal kidneys (bottom) using a confocal microscope. The arrows in the merged panel point to $CD31^+FSP1^+$ cells. (B, right) α-SMA and CD31 double labeling. The panels display representative images of kidneys that were labeled with antibodies to α-SMA (green) and CD31 (red). Yellow color in the merged panel indicates coexpression of α-SMA and CD31. (C) Quantification of fibroblasts. The bar graphs summarize average number of $FSP1^+$ fibroblasts, $CD31^+FSP1^+$ cells, α-SMA^+ fibroblasts, and $CD31^+\alpha$-SMA^+ cells per visual field in both normal and diabetic kidneys at a magnification of ×63 ($n = 3$ mice per group, 10 hpf per mouse, 30 hpf total). Magnification, ×63 in B.

was lower compared with the STZ model. This suggests that depending on the underlying cause of renal disease, specific triggers may induce varied levels of EndMT. Although EndMT is relatively well studied during embryonic development, the mechanism of EndMT in adults is not yet understood. More studies are clearly needed to address the mechanisms of EndMT in kidney fibrosis and to address whether inhibition of EndMT is a potential therapeutic strategy against renal fibrosis.

CONCISE METHODS

Animals

Seven-week-old C57BL/6 and CD1 mice were purchased from Charles River (Wilmington, MA). *COL4A3 KO* mice, *Tie2-Cre* mice, and *R26R-stop-EYFP* mice (all on a C57BL/6 background) have been described previously.[15,17,18] All mouse studies were reviewed and approved by the institutional animal care and use committee.

Method of UUO

UUO was performed on the left kidney of CD1 mice as described previously.[19] Mice were killed humanely at day 7 after UUO surgery and kidney samples were collected.

STZ Administration to CD1 Mice

We made CD1 mice diabetic by single intraperitoneal injection of STZ at 200 mg/kg in 10 mM citrate buffer (pH 4.5) at the age of 8 wk.[14] We injected citrate buffer as a control. Mice were killed at 6 mo after the injection of STZ.

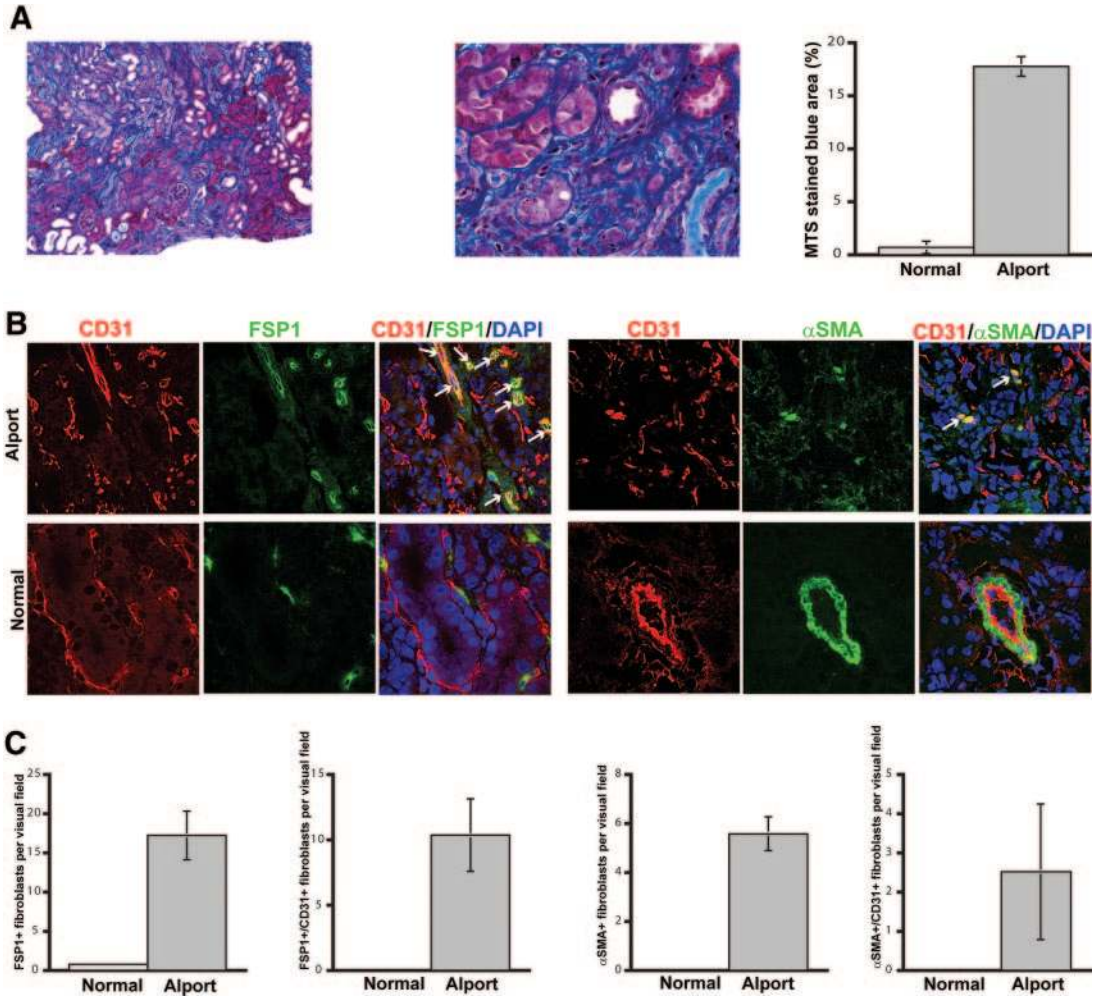

Figure 3. EndMT in *COL4A3*-deficient mice. (A) Kidneys of *COL4A3 KO* mice, a mouse model for Alport syndrome, were analyzed at the age of 22 wk. The pictures display representative photomicrographs of MTS-stained kidney sections at an original magnification of ×10 (left) and ×60 (middle). Fibrosis was digitally quantified and is shown as the percentage of MTS-stained blue area in both normal and *COL4A3 KO* kidneys (right). (B, left) FSP1 and CD31 double labeling. Kidney sections were double stained with antibodies to FSP1 (green) and CD31 (red). DAPI was used as a nuclear stain (blue). The panels display representative images that were obtained from *COL4A3 KO* kidneys (top) and normal kidneys (bottom). The arrows in the merged panel point to $CD31^+FSP1^+$ cells. (B, right) α-SMA and CD31 double labeling. The pictures display representative photomicrographs of kidneys that were labeled with antibodies to α-SMA (green) and CD31 (red). DAPI was used for labeling of nuclei (blue). Yellow color in the merged panel indicates coexpression of α-SMA and CD31. (C) Quantification of fibroblasts. The bar graphs summarize average number of $FSP1^+$ fibroblasts, $CD31^+FSP1^+$ cells, α-SMA^+ fibroblasts, and $CD31^+\alpha$-SMA^+ cells per visual field in both normal and Alport kidneys at a magnification of ×63 (n = 3 mice per group, 10 hpf per mouse, 30 hpf total). Magnification, ×63 in B.

Immunofluorescence Labeling

We cut frozen tissue into 10-μm-thick cross-sections that were fixed in 100% acetone at −20°C for 10 min. We incubated the sections with primary antibodies at 4°C overnight. The primary antibodies were rat anti-CD31 (clone MEC13.3; BD Pharmingen, San Diego, CA), rabbit anti-FSP1 (polyclonal; research gift from Eric G. Neilson, Vanderbilt University, Nashville, TN), and mouse anti–α-SMA (Sigma [St. Louis, MO] or Abcam [Cambridge, MA]). We used Alexa Fluor 488–, 568–, and 594–conjugated secondary antibodies (Invitrogen, Carlsbad, CA). We counterstained the nuclei with 4′,6-diamidino-2-phenylindole (Vectashield; Vector Laboratories, Burlingame, CA). Staining was analyzed independently by two investigators using a Zeiss LSM 510 Meta scanning confocal microscope. Ten visual fields per kidney were analyzed for co-localization of endothelial and fibroblast markers. Results are expressed as means ± SEM. With regard to the evaluation of α-SMA–positive fibroblasts, we considered only single cells that were not associated with larger vessels. To preserve the YFP signal in the *Tie2-Cre;R26R-stop-EYFP* mice, we fixed tissue in 4% PFA for 2 h, then cryoprotected it in 30% sucrose in PBS at 4°C overnight and snap-froze it in OCT. FSP1 and α-SMA staining was then performed as described already.

Quantitative Evaluation of Fibrosis

Masson Trichrome Staining was performed by the BIDMC Histology Core Facility on paraffin-embedded tissue to detect collagen

fibers. The amount of collagen deposition (blue area) was then digitally quantified using the Image-Pro Plus 6.2 (Media Cybernetics, Bethesda, MD).

ACKNOWLEDGMENTS

This study was partially funded by research grants DK62987 (R.K.), DK61688 (R.K.), DK55001 (R.K.), AA13913 (R.K.), CA12550 (R.K.), a Scientist Development Grant by the American Heart Association 0735602T (E.M.Z.), the Mentored Clinical Scientist Development Awards 1K08 CA129204 (E.M.Z.) and K08 DK074558 (M.Z.) from the National Institutes of Health, the ASN Carl W. Gottschalk Scholar Grant (M.Z.), an National Institutes of Health Cell and Developmental Biology Training Grant GM07226 (S.P.), and research funds from the Beth Israel Deaconess Medical Center for the Division of Matrix Biology.

DISCLOSURES

None.

REFERENCES

1. Harris RC, Neilson EG: Toward a unified theory of renal progression. *Annu Rev Med* 57: 365–380, 2006
2. Zeisberg M, Kalluri R: Experimental strategies to reverse chronic renal disease. *Blood Purif* 22: 440–445. 2004
3. Zeisberg M, Strutz F, Muller GA: Renal fibrosis: An update. *Curr Opin Nephrol Hypertens* 10: 315–320, 2001
4. Strutz F, Zeisberg M: Renal fibroblasts and myofibroblasts in chronic kidney disease. *J Am Soc Nephrol* 17: 2992–2998, 2006
5. Eddy AA: Molecular insights into renal interstitial fibrosis [Editorial]. *J Am Soc Nephrol* 7: 2495–2508, 1996
6. Iwano M, Plieth D, Danoff TM, Xue C, Okada H, Neilson EG: Evidence that fibroblasts derive from epithelium during tissue fibrosis. *J Clin Invest* 110: 341–350, 2002
7. Zeisberg EM, Tarnavski O, Zeisberg M, Dorfman AL, McMullen JR, Gustafsson E, Chandraker A, Yuan X, Pu WT, Roberts AB, Neilson EG, Sayegh MH, Izumo S, Kalluri R: Endothelial-to-mesenchymal transition contributes to cardiac fibrosis. *Nat Med* 13: 952–961, 2007
8. Zeisberg EM, Potenta S, Xie L, Zeisberg M, Kalluri R: Discovery of endothelial to mesenchymal transition as a source for carcinoma-associated fibroblasts. *Cancer Res* 67: 10123–10128, 2007
9. Eisenberg LM, Markwald RR: Molecular regulation of atrioventricular valvuloseptal morphogenesis. *Circ Res* 77: 1–6, 1995
10. Chevalier RL: Molecular and cellular pathophysiology of obstructive nephropathy. *Pediatr Nephrol* 13: 612–619, 1999
11. Inazaki K, Kanamaru Y, Kojima Y, Sueyoshi N, Okumura K, Kaneko K, Yamashiro Y, Ogawa H, Nakao A: Smad3 deficiency attenuates renal fibrosis, inflammation, and apoptosis after unilateral ureteral obstruction. *Kidney Int* 66: 597–604, 2004
12. Norman JT, Orphanides C, Garcia P, Fine LG: Hypoxia-induced changes in extracellular matrix metabolism in renal cells. *Exp Nephrol* 7: 463–469, 1999
13. Ritz E, Stefanski A: Diabetic nephropathy in type II diabetes. *Am J Kidney Dis* 27: 167–194, 1996
14. Sugimoto H, Grahovac G, Zeisberg M, Kalluri R: Renal fibrosis and glomerulosclerosis in a new mouse model of diabetic nephropathy and its regression by bone morphogenic protein-7 and advanced glycation end product inhibitors. *Diabetes* 56: 1825–1833, 2007
15. Sugimoto H, Mundel TM, Sund M, Xie L, Cosgrove D, Kalluri R: Bone-marrow-derived stem cells repair basement membrane collagen defects and reverse genetic kidney disease. *Proc Natl Acad Sci U S A* 103: 7321–7326, 2006
16. Iwano M, Fischer A, Okada H, Plieth D, Xue C, Danoff TM, Neilson EG: Conditional abatement of tissue fibrosis using nucleoside analogs to selectively corrupt DNA replication in transgenic fibroblasts. *Mol Ther* 3: 149–159, 2001
17. Koni PA, Joshi SK, Temann UA, Olson D, Burkly L, Flavell RA: Conditional vascular cell adhesion molecule 1 deletion in mice: Impaired lymphocyte migration to bone marrow. *J Exp Med* 193: 741–754, 2001
18. Srinivas S, Watanabe T, Lin CS, William CM, Tanabe Y, Jessell TM, Costantini F: Cre reporter strains produced by targeted insertion of EYFP and ECFP into the ROSA26 locus. *BMC Dev Biol* 1: 4, 2001
19. Zeisberg M, Soubasakos MA, Kalluri R: Animal models of renal fibrosis. *Methods Mol Med* 117: 261–272, 2005

See related editorial, "How Many Different Roads May a Cell Walk down in Order to Become a Fibroblast?" on pages 2246–2248.